Jurnal Sains Nuklear Malaysia, 2024, 36(No. 1): 62 – 80
ISSN: 2232-0946

DOSE RATE PREDICTIVE MODEL OF TERRESTRIAL GAMMA RADIATION BASED ON SUPERFICIAL-WEATHERED SOIL AND ROCKS: CASE STUDY IN SARAWAK, MALAYSIA

Hairul Nizam Idris[1,2], Mohamad Syazwan Mohd Sanusi[2], Ahmad Termizi Ramli[2], Wan Muhamad Saridan Bin Wan Hassan[2], Mohd Rafi Mohd Solleh[3], Faizal Yahaya[4], Mohd Zaini Ya'cob[3] and Wee Boon Siong[5]

[1]Waste Technology & Environment, Division,
Malaysian Nuclear Agency, Kajang, Bangi, Malaysia
[2]Department of Physics, Faculty of Science,
University Teknologi Malaysia, Skudai, Johor, Malaysia
[3]Faculty of Engineering and Life Sciences,
Department of Science and Biotechnology, University of Selangor, Malaysia
[4]Faculty of Education and Social Sciences,
Departmnet of Social Sciences, University of Selangor, Malaysia
[5]Faculty of Resource Science and Technology,
Universiti Malaysia Sarawak, Kota Samarahan, Sarawak, Malaysia
Correspondence author: hairul_nizam@nuclearmalaysia.gov.my

ABSTRACT

Estimating terrestrial gamma radiation (TGR) levels is crucial for assessing the annual effective dose received by the public due to natural radiation exposure. Cumulative doses from various sources can become significant, warranting a spatial understanding of TGR distribution. Few countries have comprehensively mapped TGR on a national scale, often facing challenges due to remote or inaccessible regions. This study explores the feasibility of estimating TGR dose rates using a linear regression model based on surface-weathered soils and rocks in Sarawak, Borneo, Malaysia. Geological studies reported that a rich diversity of rock types shaped by complex tectonic history can be found in Sarawak, predominantly sedimentary rocks covering 93% of the region, while igneous and metamorphic rocks constitute the remaining 7%. In this study, a total of 1044 TGR dose rate measurements were collected. The measurement ranges from 7 to 320 nGy h-1, with a mean of 100 nGy h-1.. Non-parametric statistical analyses of variance have validated the notable dissimilarities among six categories of superficial-weathered soil and distinguished the two distinct groupings of sedimentary and igneous rocks. The regression analysis produced a model for predicting TGR dose rates (nGy h^{-1}) = 0.992Dsoil – 0.816Drock + 109. The model showed a sufficient linear correlation, with spatial maps generated from in-situ measurements and the regression model displaying similar regional dose rate contours. Semivariogram analysis supported the model's reliability for predicting TGR dose rates in areas with similar geological backgrounds. In conclusion, this study has successfully developed a predictive model for TGR dose rates in Sarawak, based on superficial-weathered soil and rock data. While the model is specific to the Sundaland-Borneo tectonic block, it provides a valuable tool for spatial inference of TGR dose rates in unsampled locations with similar geological characteristics, aiding in radiation exposure assessment and environmental monitoring.

Keywords:Terrestrial gamma radiation, spatial dose mapping, background radiation, soil-rock gamma dose rate.

INTRODUCTION

Baseline data pertaining to regional terrestrial gamma radiation (TGR) levels is vital for estimating the annual effective dose accrued by the public due to natural radiation exposure. Although TGR-induced radiation exposure is typically low, the cumulative dose from various sources, such as medical radiation procedures, impacting the public can be substantial. In this context, the development of a spatial representation of TGR distribution is expected to provide valuable insights for assessing the potential regional public dose stemming from both anthropogenic sources, like nuclear fallout events resulting from accidents or increased nuclear weapon tests (Quindos et al., 1994; Pálsson et al., 2013; Kleinschmidt & Watson, 2015), and terrestrial contaminations associated with technologically enhanced naturally occurring radioactive materials (TENORM) linked to mining industries (AELB, 1991). Moreover, this information about regional populations exposed to radiation also plays a pivotal role in epidemiological risk assessments of diseases with hereditary links to cancer, as well as evaluating health risks associated with heightened background radiation exposure (BEIR VII, 2006; ICRP 103).

Only a handful of countries have successfully executed comprehensive TGR mapping on a national scale. For instance, Canada and the United States have undertaken such mapping endeavors under the guidance of Grasty and LaMarre (2004), Croatia through Mora et al. (2007), Spain as documented by Suarez et al. (2000), Portugal by Batista et al. (2013), Great Britain in the work of Chernyavskiy et al. (2016), Iran through Kardan et al. (2017), European countries as documented in the European Atlas of Radiation Map by Cinelli et al. (2019), China by Feng et al. (2020), and Switzerland through studies conducted by Rybach et al. (2002) and Folly et al. (2021). However, generating a comprehensive TGR distribution map necessitates an extensive in-situ gamma survey conducted on the ground, incurring substantial costs and occasionally proving time-consuming, particularly for geographically inaccessible regions (Ramli et al., 2003; Sanusi et al., 2014). The current study delves into the feasibility of estimating TGR dose rates through a linear regression model based on data from dose rates obtained from surface-weathered soils and rocks in Sarawak, Borneo, Malaysia.

According to the scientific review paper authored by Ahmad et al. (2015), all studies on terrestrial natural radioactivity in Malaysia focused solely on study locations located in Peninsular Malaysia. Meanwhile, Dodge-Wan et al. (2020) stated that previous studies conducted in Borneo were constrained to urban areas. Therefore, a research effort was initiated to carry out a more extensive study on terrestrial natural radioactivity throughout the entirety of the Borneo region in Malaysia, covering Sarawak and Sabah. This paper presents the findings of a study conducted in the state of Sarawak. Another scientific article will be devoted to the region of Sabah.

Sarawak, situated in the northwest of Borneo, constitutes one of the two states comprising East Malaysia, along with Sabah. It encompasses an area of 125,206 km^2, featuring a coastal plain and dissected uplands that can reach elevations of up to 2400 meters. The urbanization zone in Sarawak is predominantly concentrated along the coastlines, where cities and towns have burgeoned as hubs of economic and social activity. However, a significant portion of the region is characterized by vast expanses of dense jungles, highland terrain, and other challenging landscapes that remain largely untouched and shrouded in wilderness. These natural attributes contribute to the diverse and intricate geographical fabric of Sarawak, with urbanization primarily hugging the coastlines while extensive tracts of rugged terrain remain relatively pristine and cloaked in impenetrable wilderness (Agriculture Department Sarawak, 2000).

Sarawak has a wide array of rock formation types molded by its intricate tectonic history and diverse types of great soil group, as illustrated in Fig. 1 (a) and Fig. 1 (b) respectively. Most of the region (constituting 93% of the total area) is dominated by sedimentary rocks (116,676 km^2), forming a substantial part of the landscape. These sedimentary rocks, encompassing sandstones, mudstones, and shales, were deposited during various geological epochs, spanning from the Mesozoic to Cenozoic eras. Minor rock formation types (constituting approximately 7% of the total area) in Sarawak include igneous and metamorphic rocks (spanning approximately 8530 km2), contributing to the geological diversity of the region with varieties such as granite, gneisses, and schists. These rock formations were shaped during tectonic events in the Late Mesozoic and Early Cenozoic periods (Department of Mineral and Geosciences Malaysia, 1992).

Fig. 1 (a)

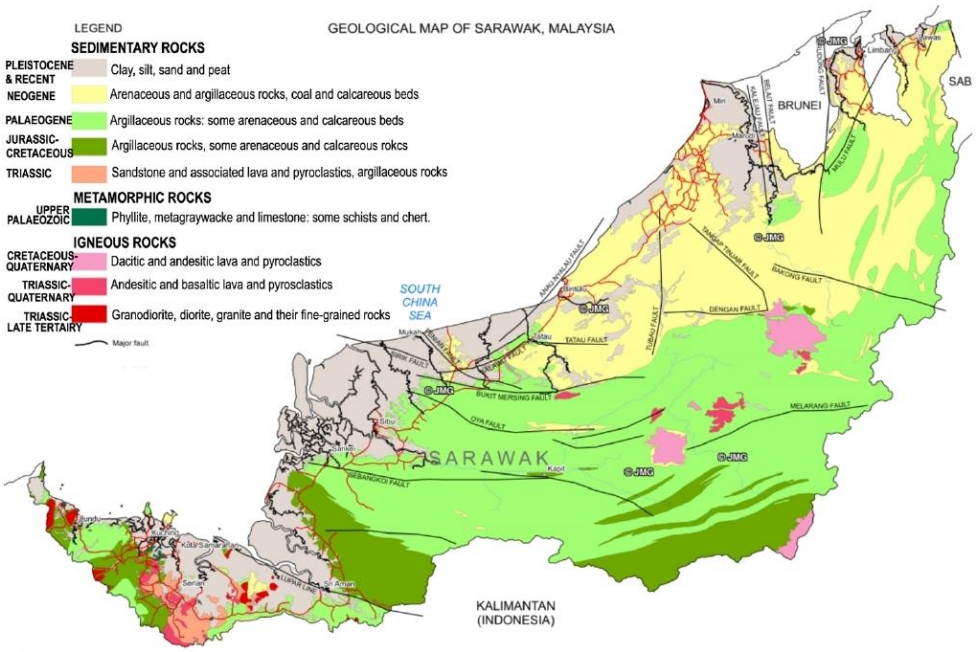

Fig. 1 (b)

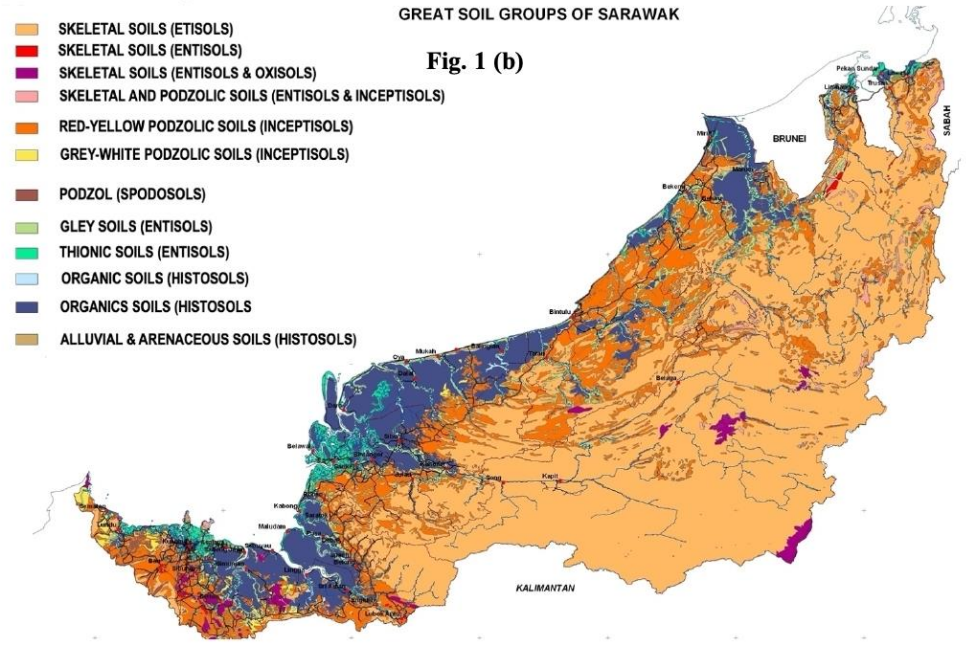

Figure 1 (a) Geological map and **(b)** soil group of Sarawak Borneo (Department of Mineral and Geosciences Malaysia, 1992; Agriculture Department Sarawak, 2000).

MATERIALS AND METHODS

Selection of the TGR survey sites

For the current study, the determination of TGR dose rate survey locations were based on two main sources of information: geological map (Department of Mineral and Geosciences Malaysia, 1992) and soil distribution maps of the Sarawak state (Agriculture Department Sarawak, 2000), as shown in Figure 1. To begin with, all the maps were digitized using ArcGIS ESRI Version 10.5 (Esri, 2017). Subsequently, approximately 1250 survey points were randomly generated, with one survey point per each 100 km², using the digitized tectonic and pedogenesis distribution maps. This procedure was carried out to ensure that the projected TGR survey points adequately covered all the weathered-soil and rock groups. For skeletal-oxisols, podzolic, and sedimentary rock groups, achieving a homogeneous distribution of survey point projections across each block was easily accomplished due to their expansive areas. Conversely, for the igneous group, gley, thionic, alluvial, and organic groups, additional survey points were plotted to ensure a sufficient sample size (above 30 sites) due to their scattered locations and limited coverage. With the assistance of topographic maps, the survey points were aligned with nearby and accessible roads. The proposed points underwent a double-check to remove survey points that may have been incorrectly located in mountainous terrain, dense forests, lakes, or inaccessible areas.

Instrument calibration

The gamma survey meter used was the Ludlum Measurement, Inc. Model 19 Micro R Meter, a scintillation survey meter manufactured in Texas, USA (Ludlum, 1993). This meter's energy detection range encompasses a wide spectrum of primordial gamma (γ) radiation emitters, including the anthropogenic γ emitter ^{137}Cs (Ludlum, 1993). With a low energy detection limit of approximately 60 keV and a typical quantum efficiency of 20–30%, the instrument's energy calibration utilized standard multi-nuclides such as ^{241}Am, ^{57}Co, ^{133}Ba, ^{137}Cs, and ^{60}Co (Ludlum, 1993), resulting in a non-linear energy response curve spanning from 59.54 keV to 1.17 MeV. The performance calibration of the instruments was carried out at the Secondary Standard Dosimetry Laboratory (SSDL) of the Malaysian Nuclear Agency, following the IEC 1017-1:1990 standards (IEC 1017, 1990), the National Physical Laboratory's dose rate meter calibration technique (BCRU, 1981), as well as IAEA Safety Standard Series No. GSG-10 (IAEA, 2018). Calibrations were performed across three exposure ranges: 0–250 μR h^{-1}, 250–500 μR h^{-1}, and 500–5000 μR h^{-1}. The calibration results were expressed in terms of dose rate using a linear equation (Eq. 1) (Sanusi et al., 2017):

$$D = B \times J \times C_f \times 8.7 \text{ nGy } \mu R^{-1} \text{ h}^{-1} \quad (1)$$

In this context, D represents the calibrated dose rate in nGy h^{-1}, B denotes the output reading (μR h^{-1}), and J represents the correction factors for each respective exposure rate range (1.00, 1.03, and 0.96). C_f is the averaged calibration factor derived from the ratio of the true value of the primary standard source to the dose rate of the uncalibrated instrument. In this study, we utilized a ^{137}Cs source emitting at 662 keV and a ^{60}Co source emitting γ energies at 1173 and 1332 keV (with an effective quantum energy of 1250 keV for ^{60}Co). For calibrating the energy dependence of the dose rate meter from environmental γ radiation sources, the British Calibration Service Publication 0811 (BCRU, 1981) has recommended the use of ^{137}Cs (662 keV) and ^{60}Co (1250 keV) as reference gamma sources. In our research, the calculated C_f values using ^{137}Cs and ^{60}Co sources were 0.95 ± 0.05 and 1.49 ± 0.03, respectively, resulting in an average calculated C_f of 1.22 ± 0.27. The acceptable C_f range for dose rate meters, as specified by ISO and IEC standards, lies between 0.8 and 1.2 (Alamares and Caseria, 1995).

To validate against internal background contributions stemming from radioactive contamination within instrument compartments or electronic noise, dose rate responses of survey meters were examined within an underground lead bunker at the Department of Physics, Universiti Teknologi Malaysia. The instruments exhibited zero-dose rate responses from internal background sources. On the cosmic response validation, the survey meters were tested on a fiberglass boat located 3 kilometers off the mainland in the middle of the sea based on technical report by British Calibration Service Publication 0811 (BCRU, 1981). The instruments displayed an inconsistent response, ranging from zero to half of the lowest scale (0 – 1.25 μR^{-1} h^{-1}), indicating weak cosmic photon components and zero response from hadronic muon showers. During fieldwork, manual stripping of the cosmic background was performed to correct the measured TGR dose rates. The measured cosmic radiation contributions (~1.25 μR^{-1} h^{-1}) absorbed dose rate in air at sea level) aligned with the measured cosmic dose rate at sea level in mid-northern latitude areas (3.67 μR^{-1} h^{-1}) (BCRU, 1981; UNSCEAR, 2000). Additionally, some of this background response might stem from gamma radiation emitted by silica material in the fiberglass boat and traces of U and Th series in seawater.

TGR dose rate measurement technique

The TGR dose rate surveys were conducted based on selected survey points during several series of fieldwork. Two instrument units were utilized to measure the TGR dose rates. Four measurements were taken at each survey point using two identical γ survey meters, positioned 1 meter above the flat, well-drained, and open soil surface, away from embankment areas, trees, outcrops, roads, pavements, and concrete foundations. The chosen site area needed to be open and free from tree canopies to avoid sites with a substantial thickness (up to 2–3 inches from the surface) of organic and humus horizon layers (based on USDA taxonomy). Measurements were performed at different spots approximately 5–10 meters apart to capture local variability in the measurements before averaging all the measured dose rate values. The fieldwork surveys were conducted during the dry seasons (March – October in 2016 and 2017) to avoid rainy days. Measurements were primarily taken from midday onwards to allow moist subsurface soil to evaporate (from morning dews) and ensure there was no self-absorption of *h* radiation in moist and wet soil, which could lead to reduced dose rate readings.

Dose rate corrections

The instrument utilized was a NaI-based detector doped with a micromole of thallium, which exhibits an overresponse to scattered and low-energy photons, effectively capturing nearly all photons passing through its crystal geometry. To address the issue of overestimated output generated by the scintillation crystal detector in this study, a correction was applied using an in situ-to-calculated dose rate ratio of 0.86. The calculated dose rates were determined by employing soil-to-air dose conversion factors (DCFs) based on soil activities of the ^{238}U and ^{232}Th series, ^{40}K, and ^{137}Cs at the locations where the in-situ dose rates were measured. These soil-to-air DCFs (measured in nGy h^{-1} per Bq kg^{-1}) were sourced from the study conducted by Sanusi et al. (2021), which utilized the MCNP5 radiation transport package for soil-to-air gamma dose simulations using a large volume of soil source. The values of soil-to-air gamma dose conversion factors used in this study are 0.349, 0.465, 0.034 and 0.067 nGy h^{-1} per Bq kg^{-1} for ^{238}U and ^{232}Th series, ^{40}K, and ^{137}Cs, respectively. In order to obtain a reliable correction factor in terms of statistics, a large sample, including both in-situ and calculated dose rates, is required. This study was conducted in conjunction with three series of fieldwork: 1) Peninsular Malaysia, Borneo region; 2) Sabah; and 3) Sarawak. A total of 468 soil samples were collected and analyzed for their activity levels of ^{238}U and ^{232}Th series, ^{40}K, and ^{137}Cs in the soils using an HPGe gamma spectroscopy system.

A large number of samples is also necessary to ensure a broad range of dose rates, from a few nGy h^{-1} up to 1200 nGy h^{-1}, thus ensuring correction across the full gamma intensity spectrum. The samples were collected randomly with the goal of covering a grid of 1000 km^2 per soil sample, and only one sample was collected at each location. Although Malaysia's total area is 330,345 km^2, this study managed to collect additional samples, especially in anomaly areas, for further study. Each sample, approximately 1.0 – 1.3 kg bulk soil, was collected at a depth of 1 – 2 ft to ensure that the calculated dose rate gives a representative value of the location. Additionally, samples were dug out in flat, well-drained, and open soil surfaces, away from embankment areas, trees, and outcrops, to ensure similar soil types and geological zones that represent an averaged in-situ TGR values of four measurements carried out at the sampling locations. The energy and efficiency calibration of the HPGe was performed using gamma emitters of precisely known energy from mix-multinuclides: ^{210}Pb, ^{241}Am, ^{109}Cd, ^{57}Co, ^{123m}Te, ^{51}Cr, ^{113}Sn, ^{85}Sr, ^{137}Cs, ^{88}Y, and ^{60}Co (Eckert & Ziegler Isotope product, 1232-2).

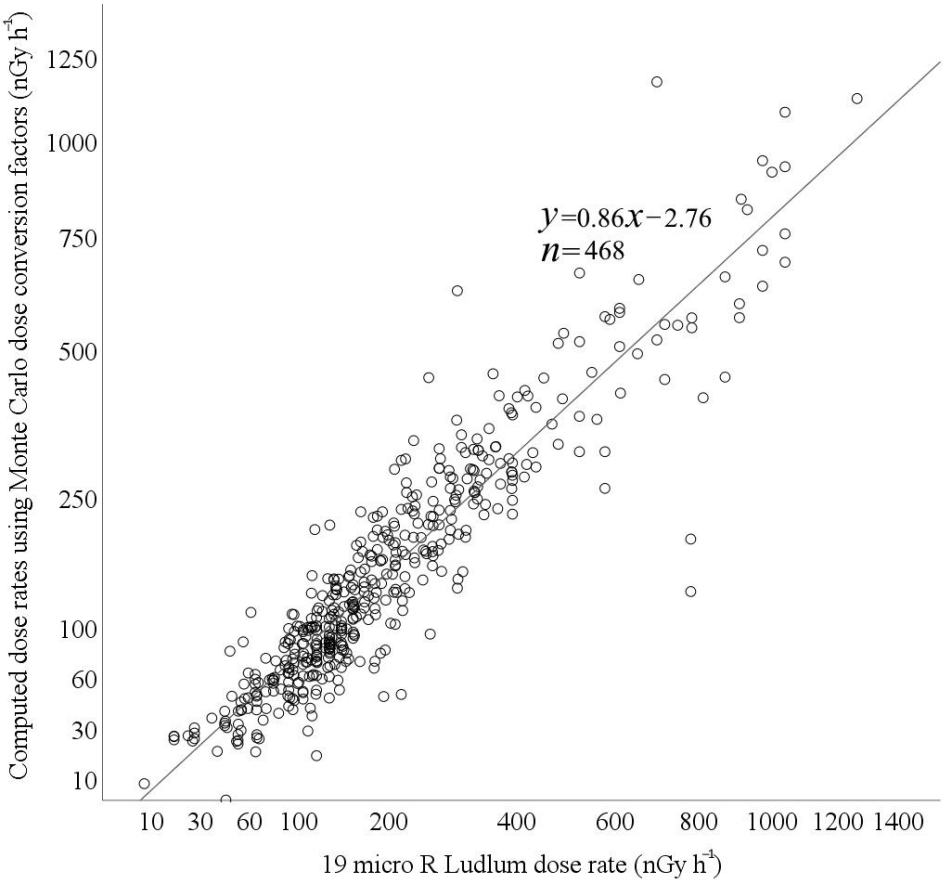

Figure 2 Survey meter dose rate correction factor of 0.86 derived from plots of Ludlum dose rates against the computed dose rates.

Figure 2 illustrates the fitted-line plots ($y = 0.86x + 2.76$ nGy h^{-1}) for instrument correction dose rates, based on computed dose rate plots compared to measurements from a Ludlum survey meter with a range of 19 micro-R. The fitted equation was employed to correct the previously overestimated dose rate readings from the Ludlum survey meter, thereby validating the gamma survey meter's suitability for assessing the high-energy range of 1332 keV to 2614 keV emanating from the ^{238}U and ^{232}Th series and ^{40}K present in the soils.

Statistical test and linear regression mode

Normality and hypothesis tests

In this study, both the Kolmogorov-Smirnov (K-S test) and the Shapiro-Wilk test (W test) were employed to numerically assess the normality distribution of the measured TGR data. Note that statistical hypothesis tests such as ANOVA-F cannot be conducted on data that does not adhere to the principles of a normal Gaussian distribution and homogeneity of data variance. Therefore, in such cases, only non-parametric tests are applicable for hypothesis testing. In this research, the statistical hypothesis tests of Welch-ANOVA, Brown-Forsythe, and Kruskal Wallis were used to examine the significant differences between each weathered soil group and geological rock groups.

Linear regression analysis

This study employed regression analysis to explore a linear model for TGR based on soil and rocks information, with the aim of quantifying the strength of the correlation between these two variables. The results obtained from this model will be used for predicting values at unsampled points. The general multiple linear regression model used is as follows:

$$y = \beta_0 x_0 + \beta_1 x_1 + \ldots\ldots\ldots + \beta_p x_p + \varepsilon = \sum_{j=0}^{p} \beta_0 x_0 + \varepsilon \quad (2)$$

where y is the dependent variable (the predicted dose rates). The regression coefficient (β_0, β_1,…..,β_p) in equation 2 are estimated from;

$$D = X\beta \pm \varepsilon \quad (3)$$

where β represent the slopes of the linear relationships between the independent variables x_o, x_1, ……, x_p (in this study, the mean dose rates for soil, D_{soil} and rock groups, D_{rock}) and the dependent variable y. D is the vector of observed dependent variable values (in this case, the measured dose rates) with a residual ε of a random error. X is the 2 × 2 matrices of independent variables, where each column represents a different survey point and each row represents a different independent variable (i.e. D_{soil} and D_{rock}) as follows (de Smith et al., 2007);

$$X = \begin{pmatrix} Dsoil_1 & Dsoil_2 & Dsoil_3 \ldots\ldots & Dsoil_{1044} \\ Drock_1 & Drock_2 & Drock_3 \ldots\ldots & Drock_{1044} \end{pmatrix} \quad (4)$$

where $D_{soil\ i}$ represents the scalar value of mean dose rate of any soil group at survey point i while $D_{rock\ I}$ represents the scalar value of mean dose rate of any geological rocks at survey point i. This matrix represents the mean doses contributed by soil and rock (from Table 1) at each of the 1044 survey points. The goal of fitting the linear regression model is to estimate the regression coefficients β that minimize the sum of squared differences between the predicted values of y (based on X and β) and the actual observed values of D (Abdullah, 1994). The percent contributions of the obtained prediction regression factors β for soil and rock impacts are calculated as follows:

$$\text{Percent contribution } \beta = \left(\frac{SS_i}{\sum SS}\right) \times 100\% \quad (5)$$

where, SS represents the squares term.

Spatial mapping of TGR

To assess the reliability of the developed dose rate predictive model, this study employed geospatial analysis through the semivariogram from the Kriging technique, comparing it with the spatial mapping of TGR dose rates obtained through in-situ measurements. The Ordinary Kriging (OK)

technique was utilized using the ESRI GIS mapping software ArcGIS to map both sets of data: (a) in-situ TGR dose rates and (b) estimated dose rates based on the developed predictive model. The Universiti Teknologi Malaysia (UTM) holds a perpetual license for ESRI ArcGIS Desktop version 10.5 (Esri, 2017). In essence, the core concept of OK involves predicting values at unsampled points by calculating a Kriging weighted average of nearby measured values, utilizing spatial autocorrelation analysis among the sampled data points. In this study, the Kriging process encompassed two key steps: a spatial covariance analysis of the sampled points was conducted by fitting a variogram, and subsequently, the weights derived from this covariance analysis were applied to interpolate dose rates at unsampled locations across the study areas. All TGR data, both observed in-situ and predicted, underwent a log transformation using the Geostatistical Wizard tool in ArcGIS. The Approximation Method option was employed to enhance the accuracy of dose rate calculations and simplify the modelling process, addressing the skewed nature of the data distribution. The ordinary Kriging was initiated with a Multiplicative Skewing Modifier set to 1, and the Base Distribution was configured as Lognormal.

RESULTS AND DISCUSSION

As shown in Fig. 3, a total of 1044 TGR dose rates were measured in this study. The TGR measurements ranges from 7 to 320 nGy h^{-1} with a mean dose rate of 100 nGy h^{-1}. Notably, the lowest TGR dose rate was observed in the peaty and organic soil zone as indicated by the blue color in the soil profile on the map (Fig. 1b), while the highest recorded dose rate, (>300 nGy h^{-1}), was associated with skeletal soil (orange colour of soil profile in (Fig. 1b). The descriptive statistics results were tabulated in Tables 1 for both variables. As shown in Table 1, the mean dose rates of measured TGR in the sedimentary and igneous are 133 ± 8 and 99 ± 1 nGy h^{-1}, respectively, whereas the mean dose rates for the weathered soil groups; skeletal (entisols), podzolic, gley, thionic, alluvial, and organic are 126±1, 96±1, 77±2, 70±4, 65±4, 40±3 nGy h^{-1}, respectively.

Table 1 Descriptive statistics of measured TGR dose rate (nGy h^{-1}) based on weathered soil group and geological rock information.

Descriptive stats.	Soil groups						Geology	
	skeletal soils (entisols)	podzolic soils	gley soils (gleysols)	thionic soils	alluvial soils	organic soils	Sedimentary	Igneous
n	448	317	130	36	30	83	1007	37
Mean ± SE	126±1	96±1	77±2	70±4	65±4	40±3	133±8	99±1
C.I. mean (95%)	123–129	94–99	73–81	61–78	57–73	34–46	116–150	97–102
Min – max	50–320	40–210	15–170	17–165	37–150	7–105	50–200	7–320
Std. deviation	30	26	22	25	21	27	51	37
Kurtosis	4	1	2	6	8	-1	4	-0.4
Skewness	0	0	0	2	2	1	1	-0.2

SE is standard error.
CI is confidence interval.

The results of TGR dose rate measurements from this study are comparable with the TGR measurements conducted by Lai et al. (1999) in Brunei, a neighboring country located to the north-east of Sarawak state. Lai et al. (1999) found that the TGR dose rates were in the range of 15–45 nGy h^{-1} for recent development soils (alluvial and organic soils) and in the range of 45 nGy h^{-1} and higher than 60 nGy h^{-1} for the sedimentary region (skeletal soil). The results from numerical tests of Kolmogorov-Smirnov and Shapiro-Wilk (P-sig.=.000) confirm that the distribution of data sampling for most groups does not follow the Gaussian normality curve. As shown in Table 2, the results from all non-parametric ANOVA (Welch-ANOVA, Brown-Forsythe, and Kruskal Wallis) indicated that the hypotheses of having similarity in mean values of TGR dose rates for each pair of weathered soil groups and 1 pair in geological rock group are rejected. The P-sig. values of 0.000 mean less than 1 in 1,000 chances of observing the identical mean rank between two different groups.

Table 2 Non-parametric ANOVA tests for statistical verification of TGR dose difference for geological and soil influence.

Hypothesis test	Geology / Soil types	Statistic[a]	Sig.
Welch	Igneous-Sedimentary	15.604	.000
	Skeletal Soils &Oxixsols - Red-Yellow/Grey-White Podzolic Soils & Podzols-Gley Soils - Thionic Soils - Alluvial and Arenaceous Soils- Organic Soils	202.858	.000
Brown-Forsythe	Igneous-Sedimentary	15.604	.000
	Skeletal Soils &Oxisols - Red-Yellow/Grey-White Podzolic Soils & Podzols-Gley Soils - Thionic Soils - Alluvial and Arenaceous Soils- Organic Soils	244.751	.000
Kruskal Wallis	Igneous-Sedimentary	16.549	.000
	Skeletal Soils &Oxisols - Red-Yellow/Grey-White Podzolic Soils & Podzols-Gley Soils - Thionic Soils - Alluvial and Arenaceous Soils- Organic Soils.	517.626	.000

a. Asymptotically F distributed

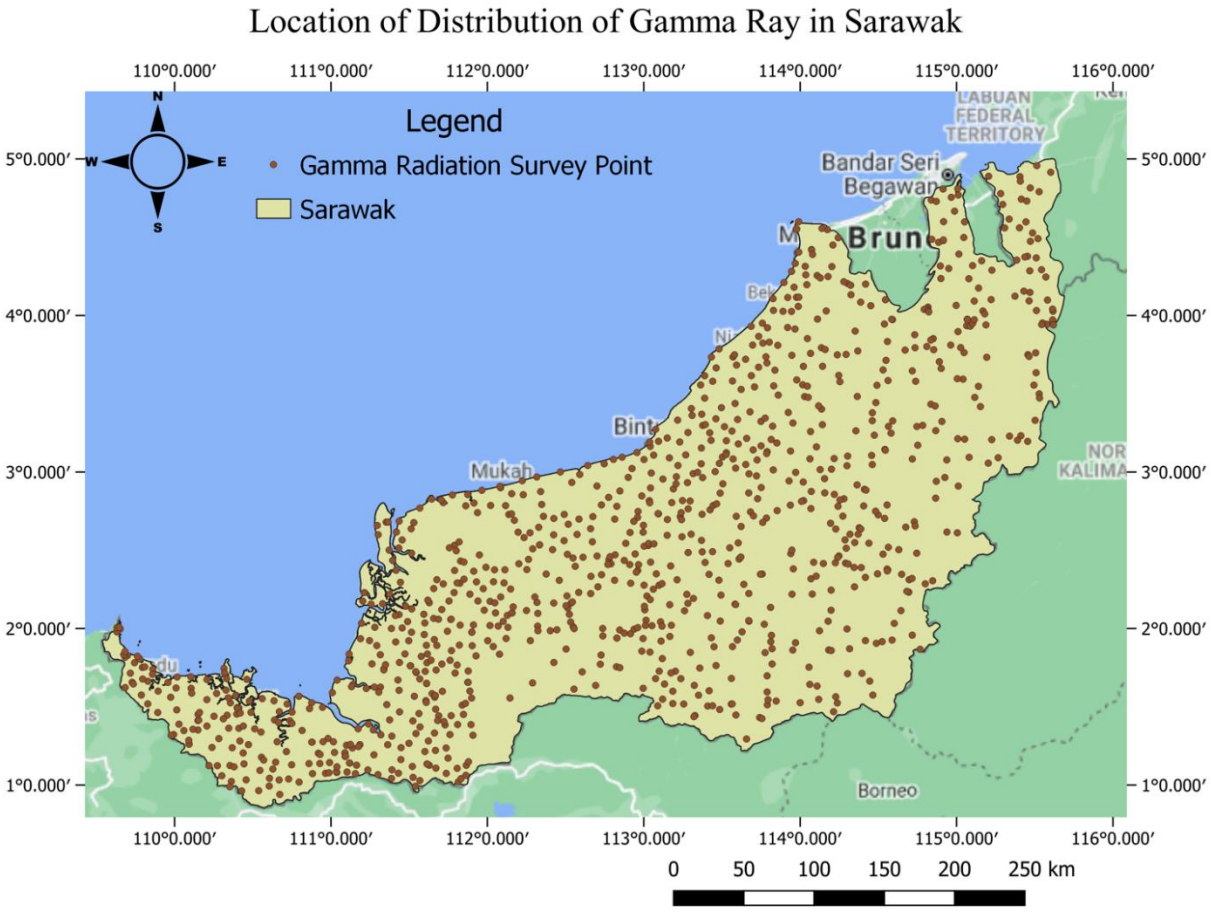

Figure 3 Distribution of TGR survey points (dots) in Borneo Sarawak.

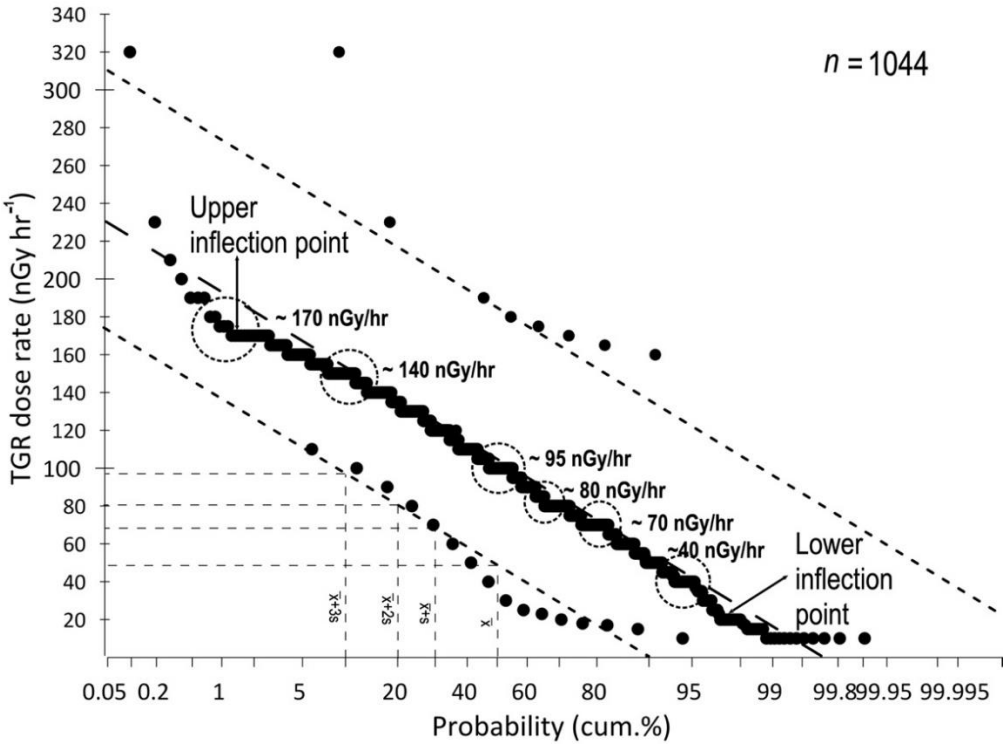

Figure 4 Sinclair's technique for cumulative probability plots of measured TGR surveys.

Figure 4 shows the graphical analysis using Sinclair's technique to examine a cumulative plot using Sinclair's technique was employed to examine the distribution of TGR dose rates across the study area. The Sinclair cumulative plot is a method commonly used in geochemistry (rare earth element, REE and other element geo-explorations) to visualize the cumulative frequency distribution of a variable (e.g. concentration of REE in sediments), in this case, TGR dose rates. The plot displays the cumulative percentage of measurements below a certain dose rate threshold on the y-axis, plotted against the dose rate threshold on the x-axis. Ideally, in a Sinclair cumulative plot, the data points would fall along a straight line, indicating a uniform distribution of dose rates. However, deviations from this straight line, as observed in our plot, suggest the presence of distinct TGR ranges at specific dose rate intervals. In our study, deviations were noted at intervals corresponding to 40, 70, 80, 95, 140, and 170 nGy h^{-1}, indicating the presence of distinct geological or environmental factors influencing TGR levels at these points. Furthermore, deviations beyond 170 nGy h^{-1} may suggest anomalous TGR readings, which could be attributed to extreme weathering processes or the accumulation of uranium-thorium-bearing heavy minerals such as zircon, ilmenite, monazite, and cassiterite, as reported in previous studies (Teh and Julius, 2002; Yokoyama et al., 2015; Hall and Breitfeld, 2018).

The differences in the mean values and variance distributions from the statistical results have numerically verified the impacts of superficial-weathered soils and geological rocks on TGR dose levels. The mean CIs in Table 1 shows that the sedimentary (116–150 nGy h^{-1}) has a higher dose rate compared to igneous (97–102 nGy h^{-1}). Unlike the igneous granitic batholiths of Peninsular Malaysia (Banjaran Titiwangsa), the Borneo's igneous existed in isolated zones primarily consisting of extrusive types i.e., dacitic, andesitic, basalts, granodiorite, and diorite. The existence of these extrusive volcanic rocks, including mafic plutonic types (e.g., granodiorite and diorites), has been identified to contain lower radioactivity compared to plutonic rocks due to their moderate acidic geochemical properties, low density, low SiO_2 content, and physical darkness in color (NCRP, 1987; Schlumberger, 1982; Azman, 2005).

Skeletal soil (entisols) shows the highest mean dose rate and CI (123–129 nGy h^{-1}) owing to its limited development and weathered products. The layers comprise unweathered parent material, such as rocks and gravel of sedimentary rocks with little or no organic matter accumulation (Agriculture Department, Sarawak 2000). This preserved the most abundant uranium (U) and thorium (Th) in the soil body compared to other weathered soil groups. The mean C.I of 123–129 nGy h^{-1} is slightly lower than the mean CI dose rate of sedimentary and metamorphic soil found in Peninsular Malaysia (152–162 nGy h^{-1}) (Sanusi et al., 2017) owing to its sedimentary content (arenaceous and calcareous) of the continental crust of Sundaland whereas the latter are from the terrane blocks derived from Gondwana which is associated with voluminous S-type granitic batholiths and belts.

Podzolic soils show the second-highest mean dose rate and CI (94 – 99 nGy h^{-1}) due to its partial association of parent materials. The soil is characterized by its moderate weathering processes and leaching process of upper horizon layers. The soil sometimes remains undifferentiated from the entisols or skeletal soils due to their similar lithological setting and the degree of parent material association (Agriculture Department, Sarawak 2000). Similarly, gleysols and thionic soils share comparable means (77 and 70 nGy h^{-1}, respectively) and CI of dose rates (73–81 and 61–78 nGy h^{-1}, respectively) due to their similarities in terms of high waterlogged conditions and anaerobic environments (FAO-UNESCO, 1974; Agriculture Department, Sarawak 2000).

These characteristics promote continuous and alternating mineral leaching conditions, including the U and Th nuclides and K from the soil bodies. As expected, the alluvial and organic soils indicate low dose rate ranges (CI range 34–73 nGy h^{-1} for both groups) owing to their rapid hydrolysis

weathering process, leading to the breakdown of NORM minerals and various physicochemical changes, alterations in texture, and porosity. Contrastingly, the transported soil bodies (alluvial or riverine soils) usually show high dose rates owing to the U and Th sedimentation process by a transported agent of water (watercourse or river) from the uphill granitic ranges to the downhill alluvial soil zones (Sanusi et al., 2014, 2017). However, due to lower U and Th nuclide series and K activities in the uphill sedimentary (skeletal) parent materials compared to the Peninsula's uphill granitoids, the impact of U and Th sedimentation is insignificant for the study area. The organic soils (CI range 34–46 nGy h^{-1}) are expected to have insignificant contribution to high doses owing to the soil's decomposed organic materials mainly from plants, which continuously degraded and solidified by heat and wind. Since most of these organic soil settings are located along the coastal plains, estuaries, and floodplains, the U and Th are expected to be diluted and dispersed by the water bodies.

Table 3 The linear regression model of TGR dose rate based on weathered soil groups and geological rock groups.

Model		Unstandardized Coefficients		Standardized Coefficients		
		B	Std. Error	Beta	*t*	Sig.
1	(Constant)	108.576	17.915		6.061	.000
	rock	-.816	.132	-.133	-6.161	.000
	soil	.992	.031	.697	32.219	.000

a. Dependent Variable: dose

As shown in Table 3, we chose the unstandardized regression coefficients (β coefficients) to represent the prediction model or direct change based on raw values (or original units) instead of standardized coefficients, which express the relative effects in terms of standard deviations or regardless of original units. The TGR dose rate predictor model consisted of one positive predictor variable (0.992 for weathered soil) and one negative predictor variable (-0.816 for geological rocks). A negative beta coefficient is observed suggests an inverse relationship between the predictor (geological rocks) and response variables (TGR dose rate), holding soil variable constant. The developed linear independent variable model based on the estimator coefficients (dependent variables) can be expressed as;

$$\text{TGR dose rate (nGy h}^{-1}) = 0.992D\text{soil} - 0.816D\text{rock} + 109 \quad (5)$$

where 109 nGy h^{-1} is a constant.

Table 4 Residual analysis of the linear model using Pearson's test (*R*) and Durbin-Watson's autocorrelation test

Model	R	R Square	Adjusted R Square	Std. Error of the Estimate	Change Statistics					
					R Square Change	F Change	df1	df2	Sig. F Change	Durbin-Watson
1	.717[a]	.514	.513	26.516	.514	550.281	2	1041	.000	1.340

a. Predictors: (Constant), soil, geo
b. Dependent Variable: dose

To assess the precision of the linear model, the auto-correlation tests based on Durbin-Watson's and Pearson's R tests were performed using the model residuals (errors). The results in Table 4 show that the calculated R-value is 0.717 whereas Durbin-Watson's statistic is 1.34. R is a multipole correlation coefficient and represents the strength of the association between the two variables. Weathered soil and rock variables shared values of 0.717, thus indicating a sufficient linear correlation. Meanwhile, Durbin-Watson value 1.34 indicated a positive correlation among residuals, thus exhibiting a systematic pattern of positive relationships.

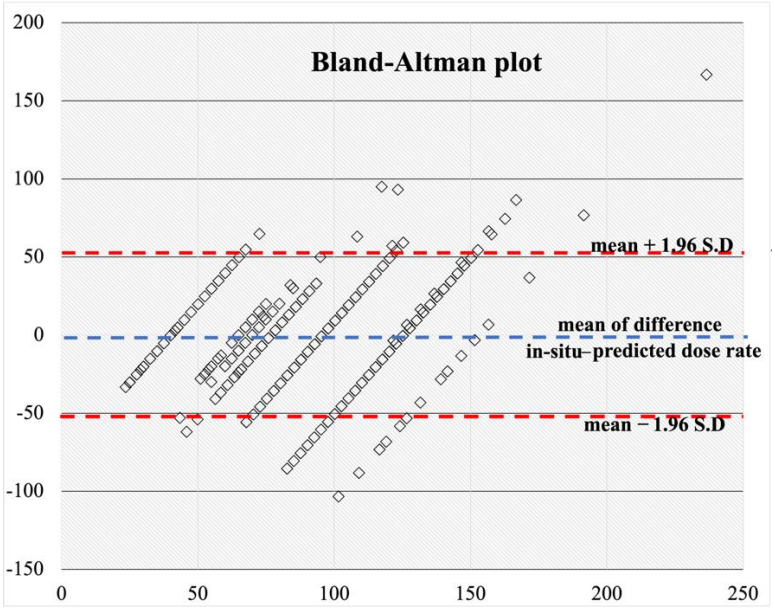

Figure 5 A Bland-Altman plot presents a direct comparison based on the mean differences of in-situ dose rates (in-situ - predicted) against the average values.

For a more direct comparison of in-situ dose rates against the predicted dose rates based on the developed regression model, a Bland-Altman plot was presented in Fig. 5. This plot illustrates the mean differences of in-situ dose rates (in-situ - predicted) against the average values between in-situ and predicted dose rates. For this purpose, all data were log-transformed to achieve a more normally distributed distribution. As depicted in Fig. 5, the average difference (or bias) obtained is -0.49 (indicated by the blue dashed line), with upper and lower limits of agreement (LOA) of 51.43 and -52.42, respectively. Most of the plots demonstrate good agreement, with approximately 95% falling within ±2 standard deviations (σ). In regions below the lower LOA, where negative values occur, the predicted dose rates appear to be overpredicted compared to the measured in-situ dose rates. Conversely, outliers above the upper LOA suggest that the predicted dose rates are underestimated compared to the in-situ dose rates. Based on this comparison, it is expected that approximately 95% of the differences between in-situ and predicted dose rates will fall within the limits of agreement.

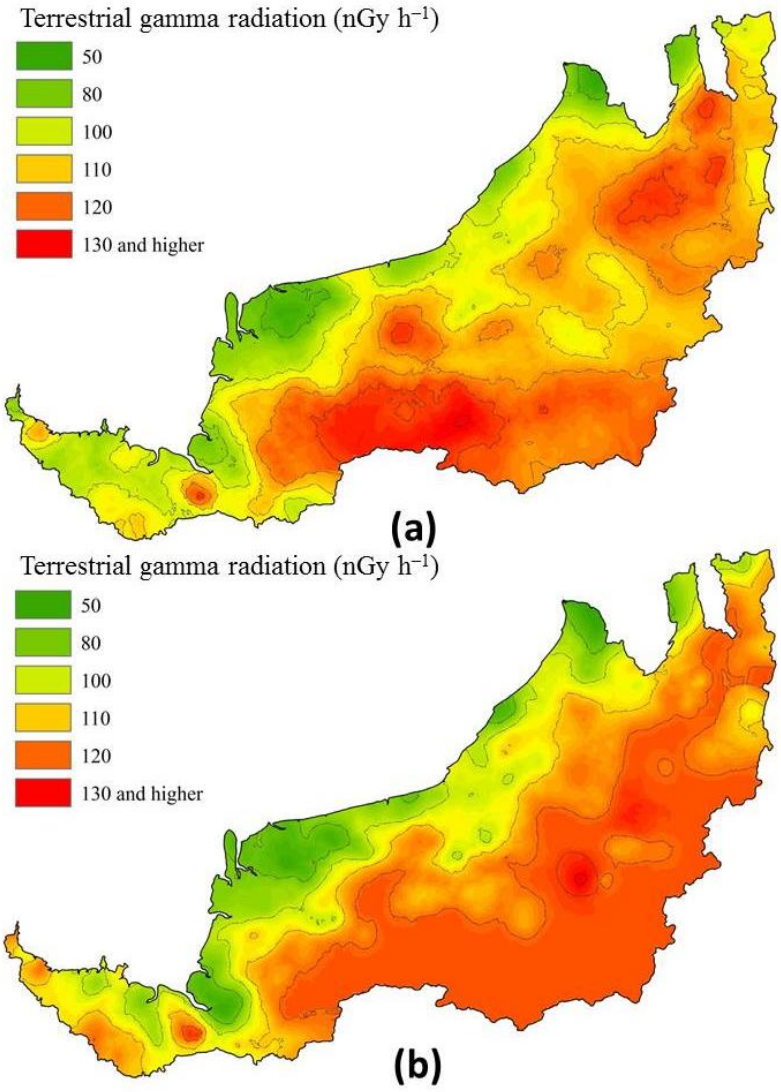

Figure 6 Distribution of TGR dose rates in Borneo Sarawak based Ordinary Kriging of (a) in-situ TGR dose rate and (b) linear regression dose predictive model.

Figure 6 shows two spatial maps of TGR dose rates developed based on: (a) in-situ TGR dose rate and (b) linear regression dose predictive model. Graphically, the maps showed similarities in terms of regional dose rate contour, where50 nGy h^{-1} to 100 nGy h^{-1} dose rate dominated the coastal and recent rock developments i.e. Quaternary and Pleistocene age of rock regions (gleysols, thionic, alluvial, and organic), whereas the upper dose rate range 110 – 320 nGy h^{-1} dominated the sedentary formation (e.g., skeletal and podzolic). To analyze the variability of these spatial maps, two semivariogram plots analysis were given in Fig. 7.

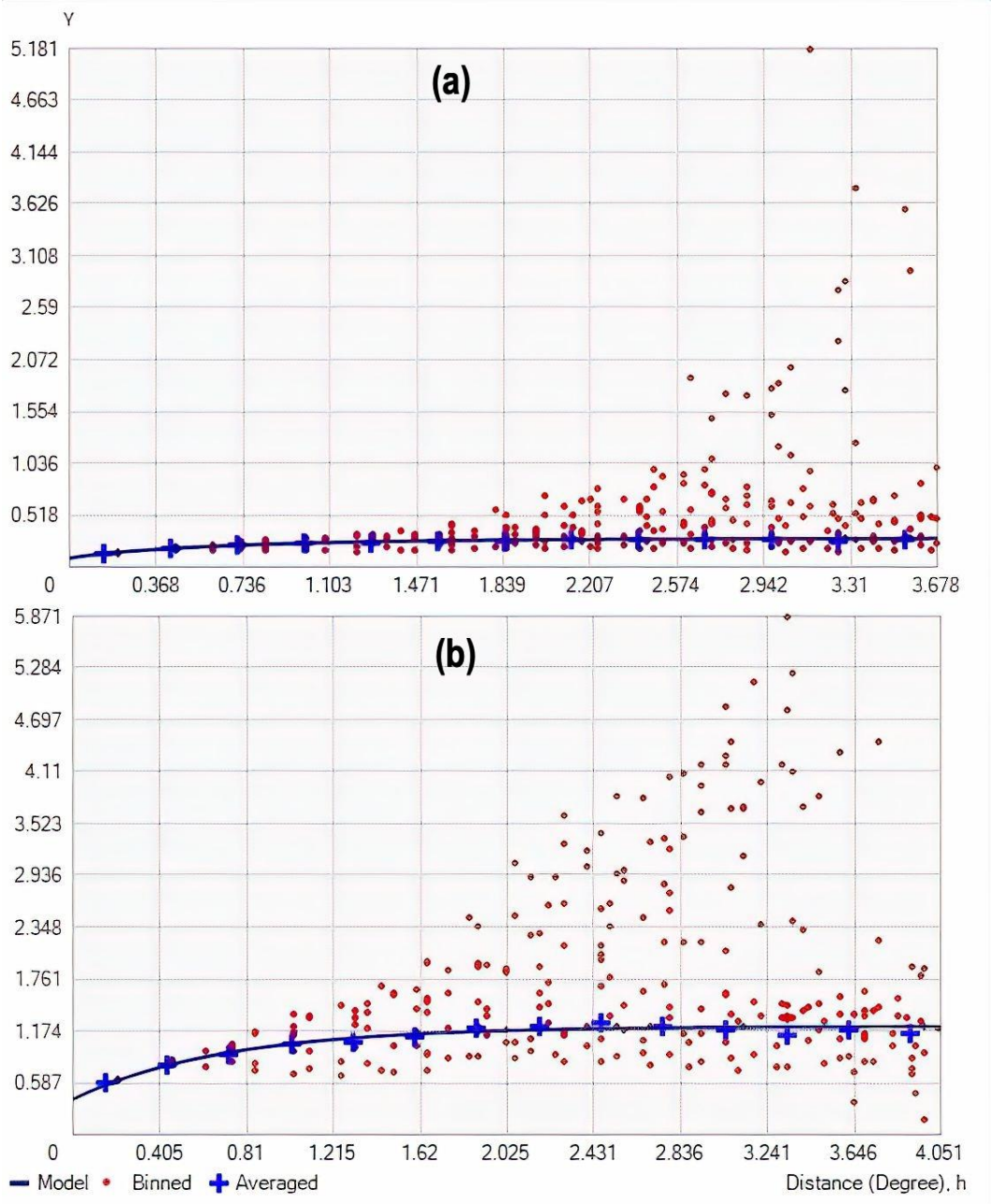

Figure 7 Semivariogram model of Kriging interpolation for comparison between (a) in-situ and (b) predicted TGR dose rates.

The semivariogram model based on a linear regression predictive model suggests that the correlation between data points decreases and eventually becomes flat (i.e., no longer correlated) at a distance of approximately 1.62 degrees. In contrast, the in-situ data indicates that the correlation between data points decreases and becomes flat at a distance of around 1.47 degrees. Comparable sill and nugget values indicated from both semivariogram plots suggest that the developed regression prediction model provides an adequate estimator for TGR dose rate prediction. Such prediction and its consistent variation are considered acceptable at environmental levels, allowing one to build an empirical, methodological basis for spatial inference. The presented model also applicable for long-term use and will not be affected by heavy rainfall and flood. For tropical climates, soil develops slowly over millions of years, and the weathering process by rain, flood, and climates may require a long time to alter the U, Th, and K distribution in soil bodies (Sanusi et al., 2017).

CONCLUSION

The study has successfully developed a regional predictive model for TGR dose rate based on information of superficial-weathered soil and rocks using linear regression model. Statistical non-parametric analyses of variance confirmed that 6 groups of weathered soils are significantly different to each other as well as two distinctive groups of sedimentary and igneous rocks. The model expressed as TGR dose rate (nGy h^{-1}) = $0.992D_{soil} - 0.816D_{rock} + 109$ only applicable for TGR dose rate for similar rock and soil types of Sundaland-Borneo. tectonic blocks of Sundaland-Borneo. Even though the model predicting the unsampled values based on the random process of sampled or nearby points (this is somehow not certainly true for any random sampled environmental data), however, it is somewhat acceptable and permits one to build an empirical methodological basis and insights for the spatial inference of TGR dose rate levels in unmeasured locations based on similar weathered soil and rock types.

ACKNOWLEDGEMENTS

This research received support from the e-Science Fund (03-01-06-SF1277) by the Ministry of Science, Technology, and Innovation, Malaysia, as well as the Fundamental Research Grant Scheme (FRGS) FRGS/1/2019/STG02/UNISEL/03/1 from the Malaysian Ministry of Higher Education. We would like to extend our sincere gratitude to the Department of Mineral and Geosciences Malaysia, Nuclear Agency Malaysia, and Universiti Teknologi Malaysia for their invaluable facilities and support. Special thanks are also due to Mr. Arbaani Akum for his assistance during fieldwork.

REFERENCES

Abdullah, M., 1994. Regression Analysis, 1st Edition. Dewan Bahasa dan Pustaka, Kuala Lumpur

AELB, 1991. Radiological hazards assessment at mineral processing plants in Malaysia. Atomic Energy Licensing Board of Malaysia. LEM/LST/ I6, Internal Report [In Malay].

Agriculture Department Sarawak, 2000. Great soil groups of Sarawak. Agriculture Department Sarawak, Kuching, Sarawak.

Ahmad, N., Jaafar, M. S., Bakhash, M., & Rahim, M., 2015. An overview on measurements of natural radioactivity in Malaysia. Journal of radiation research and applied sciences, 8(1), 136-141.

Alamares and Caseria (1995). Proceeding of the IAEA/CRA workshop on calibration of dosimeters & survey instrument for photons. Japan Atomic Energy Research Institute, 28 November – 2 December 1994, Tokai, Japan.

Azman, A.G. 2005. Geochemical characteristics of S- and I-Type Granites: Example from Peninsular Malaysia granites. Geological Society of Malaysia Bulletin 51, 123–134.

Batista, M.J., Torres, L., Leote, J., Prazeres, C., Saraiva, J., Carvalho, J. 2013. Carta Radiométrica de Portugal (1:500 000) 978-989-675-027-5, Laboratório Nacional de Energia e Geologia Governor de Portugal.

BCRU, 1981. A Guide to the Measurement of Environmental Gamma-ray Dose Rate. British Committee on Radiation Units and Measurements. National Physical Laboratory, United Kingdom, 7, 9, 0.

BEIR VII, 2006. The Biological Effects of Ionizing Radiation VII. *Health risks from exposure to low levels of ionizing radiation*. Washington, D.C.: The National Academy of Sciences.

Chernyavskiy, Kendall, G.M., Wakeford, R., Little, M.P., 2016. Spatial prediction of naturally occurring gamma radiation in Great Britain. J. Environ. Radioact.,164, 300-311.

Cinelli, G., Tollefsen, T., Bossew, P., Gruber, V., Bogucarskis, K., De Felice, L., De Corta, M., 2019. Digital version of the European Atlas of natural radiation. J. Environ. Radioact 196, 240–252

De Smith, M. J., Goodchild, M.F. dan Longley, P.A. 2007. Geospatial analysis: a comprehensive guide to principles, techniques and software tools; regressions method in Chapter 5; data exploration and spatial distribution. pp 239-241. Leicester: The Winchelsea press.

Department of Mineral and Geosciences Malaysia, 1992. Geological map of Sarawak. Department of Mineral and Geosciences Malaysia, Kuala Lumpur, Malaysia.

Dodge-Wan, D., & Mohan Viswanathan, P., 2021. Terrestrial gamma radiation dose rate mapping and influence of building materials: case study at Curtin University campus (Miri, Sarawak, Malaysia). Journal of Radioanalytical and Nuclear Chemistry, 328(1), 163-180.

Esri, 2017. ArcGIS Desktop: Release 10.5. Redlands, CA: Environmental Systems Research Institute.

FAO-UNESCO, 1974. United Nations Educational, Scientific and Cultural Organization. FAO/UNESCO Soil map of the world. Paris: UNESCO.

Feng,W., Zhang, Y., Li, Y., Wang, P., Zhu, C., Shi, L., Hou, X., Qie, X., 2020. Spatial distribution, risk assessment and influence factors of terrestrial gamma radiation dose in China. J. Environ. Radioact 222, 106325.

Folly, C.L., Konstantinoudis, G., Mazzei-Abba, A., Kreis, C., Bucher, B., Furrer, R., Spycher, B.D., 2021. Bayesian spatial modelling of terrestrial radiation in Switzerland. J. Environ. Radioact 233, 106571.

Grasty, R.L., LaMarre J.R., 2004. The annual effective dose from natural sources of ionising radiation in Canada. Radiation Protection Dosimetry. 108 (3):215 – 26.

Hall, R and Breitfeld, H.T., (2018). The eastern Sundaland margin in the latest Cretaceous to Late Eocene: Sediment provenance and depositional setting of the Kuching and Sibu Zones of Borneo. Gondwana Research 63, pp. 34 – 64.

IAEA GSG-10 2018. Prospective Radiological Environmental Impact Assessment for Facilities and Activities. IAEA Safety Standards Series No. GSG-10. International Atomic Energy Agency, Vienna.

ICRP 103, 2007. Recommendations of the international commission on radiological protection. In: International Commission on Radiological Protection ICRP Publication 103, Annals of the ICRP 37. Pergamon Press, Oxford.

IEC 1017 (1990), International Electrotechnical Commission. Portable, transportable, or installed X or gamma radiation ratemeters for environmental monitoring. Part 1: Ratemeters. IEC Standard 1017, Geneva (1990).

Kardan, M.R., Fathabdi, N., Attarilar, A., Esmaeili-Gheshlaghi, M.T., Karimi, M., Najafi, A., Hosseini, S.S., 2017. A national survey of natural radionuclides in soils and terrestrial radiation exposure in Iran. J. Environ. Radioact. 178–179, 168–176.

Kleinschmidt, R., and Watson, D., 2016. Terrestrial gamma radiation baseline mapping using ultra low-density sampling methods. J. Environ. Radioact.,151 (3), 609-622.

Lai, K.K., Hu, S.J., Minato, S., Kodaira, K., and Tan, K.S. (1999). Terrestrial gamma ray dose rates of Brunei Darussalam. Applied Radiation and Isotopes. 50 (3), 599-608

Ludlum, 1993. Instruction Manual of Ludlum Model 19 Micro R Meter. Ludlum Measurements, Inc, Texas.

Mora P., Picado, E., Minato S. 2007. Natural radiation doses for cosmic and terrestrial components in Costa Rica. App. Radiat. Isot. 65 (1), 79-84.

NCRP. National Council on Radiation Protection and Measurements 1987. Exposure of the Population in the United States and Canada from Natural Background Radiation. NCRP Report No. 45.

Pálsson, S.E., Howard, B.J., Bergan, T.D., Paatero, J. Isaksson, M. dan Nielsen, S.P. 2013. A simple model to estimate deposition based on a statistical reassessment of global fallout data. J. Environ. Radioact., 121, 75 – 86.

Quindós, L.S., Fernández, P.L., Soto, J., Ródenas, C., dan Gómez, A.J. (1994). Natural radioactivity in Spanish soils. Health Phys. 66 (2), 194–200.

Ramli, A.T., Abdul Rahman, A.T., Lee, H.M., 2003. Statistical prediction of terrestrial gamma radiation dose rate based on geological features and soil types in Kota Tinggi district, Malaysia. Appl. Radiat. Isot. 59 (6) 393 – 405.

Rybach, L., B¨achler, D., Bucher, B., Schwarz, G., 2002. Radiation doses of Swiss population from external sources. J. Environ. Radioact. 62 (3), 277–286.

Sanusi, M.S.M, Ramli, A.T., Said, M.N., Izham, A., Lee, M.H., Heryanshah, A., dan Wagiran, H. 2017. Assessment of impact of urbanisation on background radiation exposure and human health risk estimation in Kuala Lumpur, Malaysia. Environ. Int. 109, 91 – 101.

Sanusi, M.S.M., Ramli, A.T., Gabdo, H.T., Garba, N.N., Heryanshah, A., Wagiran, H., Said, M.N., 2014. Isodose mapping of terrestrial gamma radiation dose rate of Selangor state, Kuala Lumpur and Putrajaya, Malaysia. J. Environ. Radioact. 135, 67 – 74.

Sanusi, M.S.M, Hassan, W.M.S.W., Hashim, S., Ramli, A.T. (2021). Tabulation of organ dose conversion factors for terrestrial radioactivity monitoring program. Appl. Radiat. Isot. 174, 109791.

Schlumberger, 1982. Natural Gamma Ray Spectroscopy: Essentials of N.G.S. Interpretation. (unspecified).

Suarez, E., Fernandez, J. A., Baeza, A., Moro, M. A., Garcı´a, D., Pozo, J. M. and Lanaja, J. M. (2000). Proyecto MARNA. Mapa de radiacio´n gamma natural. INT-04.02 (Madrid:CSN).

Teh, G.H., and Julius, D.O.A. (2002). EPMA study of heavy minerals in the Annah Rais-Bayur area, Sarawak. Bulletin of the Geological Society of Malaysia 45. Geological Society of Malaysia Annual Geological Conference 2002.

UNSCEAR, 2000. United Nations Scientific Committee on the Effects of Atomic Radiation. Report to the general assembly. Annex B: exposures from natural radiation sources. (NY: UNSCEAR), ISBN-10: 9211422388 (2000).

Yokoyama, K., Tsusumi, Y., Bong, W.S.K., (2015). Age distributions of monazites in the Late Cretaceous to Late Eocene turbidite from northwestern Borneo and its tectonic setting, Bull. Natl. Mus. Nat. Sci., Ser. C, 41, pp. 29–43.